VIBRATION FATIGUE ANALYSIS OF COMPONENTS ON ROTATING MACHINERY UNDER SINE AND SWEPT-SINE-ON-RANDOM LOADING

A Halfpenny, F Kihm, R Plaskitt,
HBM-Prenscia, Technology Centre, Brunel Way, Rotherham S60 5WG, UK

ABSTRACT

This paper describes an approach for calculating the high-cycle fatigue life of a component subjected to sine-on-random loading. The calculation method is based on a spectral approach in the frequency-domain. This offers significant advantages over the time-domain approach when finite element analysis calculation times become prohibitive. A statistical Rainflow cycle histogram is derived directly from a sine-on-random spectrum of stress. The cycles are applied to an appropriate material fatigue curve in order to obtain the estimated life. A case study is presented to illustrate the method using a component attached to a helicopter. Comparisons with traditional time-domain approaches are presented and show excellent agreement. The paper concludes by showing how this method was extended to cover the case of swept-sine-on-random excitation.

KEYWORDS

Sine-on-Random, Swept-Sine-on-Random, Random Vibration, Vibration, Frequency-domain, Power Spectral Density (PSD), Finite Element Analysis (FEA), Rainflow Cycle Count, Fatigue Analysis.

INTRODUCTION

Sine-on-random excitations are typically generated by rotating machinery. The term ‘sine-on-random’ implies a series of sinusoidal tones, usually harmonics of the rotation speed, superimposed on a background of random noise. Pure sine-on-random excitations are seen during constant-speed rotation, while swept-sine-on-random excitations are seen during variable-speed rotation.

Long-term exposure of equipment to vibration gives rise to microscopic cracks that eventually propagate to failure; a failure mode referred to as ‘Fatigue’. Equipment is tested and qualified against fatigue failure to standards such as MIL-STD-810G [1], Def Stan 00-35 [2] and RTCA/DO160G [3]. So far, the only way of estimating fatigue life from a sine-on-random excitation is to perform a transient finite element analysis in the time-domain. The time signal is constructed by superimposing sinusoidal harmonics on a time-domain realization of the random PSD (Power Spectral Density function). Such analyses are often accelerated by using modal superposition but are still very demanding in terms of CPU time. It also raises the question of how long the excitation signal should be in order to ensure convergence on fatigue life. The time-domain approach is therefore impractical and this is the main reason why a spectral approach is relevant.

Spectral methods of estimating fatigue damage in the frequency-domain are well established. Bendat [4] published a report showing how the Rayleigh distribution could be used to estimate the fatigue cycles in a narrow-band random process. Steinberg [5] demonstrated how the Gaussian-normal distribution could be used in the case of a broad-band process. Dirlik [6] and Bishop [7] describe the derivation of an empirical probability distribution that is suitable over a range of bandwidths. And Lalanne [8] provides an analytical probability distribution based on Rice's [9] distribution of peaks in a random signal. All these methods are summarised by Halfpenny and Kihm [10] along with a comparison study of these methods with reference to the time-domain process of 'Rainflow' cycle counting.

A limitation with all these spectral methods is that they require the underlying time signal of stress to be 'Stochastic'. This implies that its amplitude statistics are 'Stationary, Ergodic and Gaussian Random'. In practice this means that the 'phase' content of the random signal is also random and can consist of any phase angle with equal probability. This assumption is necessary for many reasons, not least because the loads are often expressed in the form of a PSD.

A PSD contains information on the amplitude and frequency content of a signal, but it does not contain information on the 'phase' content. By definition a sinusoidal signal is 'Deterministic' and not 'Stochastic'. It has a finite 'phase' angle and its amplitude is not random. Although it is possible to calculate the PSD of a sine-on-random signal, this PSD alone does not offer a complete representation of the signal. This is because the phase content is missing and it cannot be approximated by a random value. Any attempt to calculate the fatigue cycles based on a Stochastic assumption is likely to underestimate the actual damage. This is because the sinusoidal tones present in the PSD representation would be interpreted as narrow-band random processes. In this case, the narrow-band processes would share the same RMS (Root Mean Square) amplitude as the sinusoidal tones but would not have the same peak amplitude. The purpose of this paper is to derive a new probability distribution in order to determine the fatigue cycles present in a sine-on-random signal.

METHODOLOGY

This section describes an approach for computing the fatigue life, or damage, of a component subjected to sine-on-random loading. The loading definition is expressed as a PSD of the random background signal along with a table of the sinusoidal frequencies and their amplitudes. The derivation starts with a brief summary of fatigue estimation in the time-domain before continuing to the new spectral approach. It concludes with a discussion on how this method may be extended further to consider the case of swept-sine-on-random loading.

Review of stress-life (SN) fatigue analysis in the time-domain

The starting point for any fatigue analysis is the response of the structure or component. In the time-domain this is usually expressed as a stress or strain time signal as illustrated in Fig. 1. Fatigue occurs as a result of stress or strain reversals in the time history. These are known as cycles. The significant aspects of these are the amplitude and the mean stress in the cycle. Today this information is extracted from the time signal using a procedure known as 'Rainflow Cycle Counting'. Matsuishi and Endo [11] first introduced the concept of Rainflow amplitudes to the scientific community in 1968 and a description of the modern Rainflow algorithm is given by Downing and Socie [12].

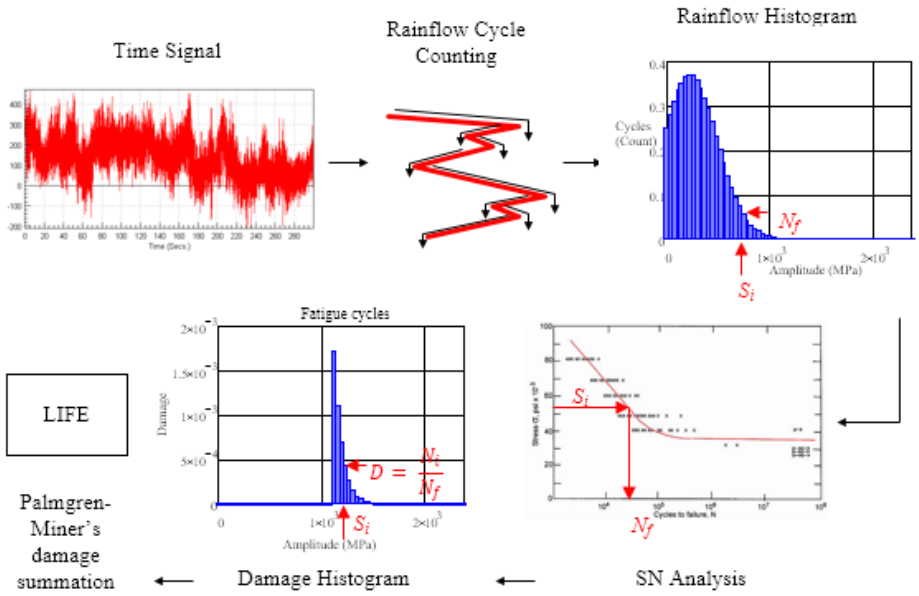

Fig 1: Time-domain fatigue analysis

In the case of vibration-induced fatigue, the mean stress of a cycle can be attributable to two factors, these are: 1) the cycle mean stress, and 2) the residual mean stress in the component.

In the case of the cycle mean stress, the effects on fatigue are relatively small because most vibration-induced loads are driven by acceleration which tends to be a zero-mean process. Therefore the effect of tensile mean cycles are largely offset by the effect of compressive cycles.

In the case of residual mean stresses in the component, these can be accounted for using traditional R-ratio correction methods such as Goodman's relationship [13] for example.

The output from a Rainflow cycle counting exercise is expressed as a 'Rainflow histogram' showing the number of cycles vs. the stress amplitude. Each cycle will induce a certain amount of fatigue damage on the component and this is quantified with a fatigue curve similar to the SN curve illustrated. The total damage over the entire test is obtained by summing the damage in each bin of the Rainflow histogram. This approach is known as the 'Palmgren-Miner accumulated damage rule', [14][15].

The damage caused by each cycle is calculated with reference to the material life curve, in this case the SN curve. The SN curve shows the number of cycles to failure, N_f, for a given stress amplitude, S. The total damage caused by N number of cycles is therefore obtained as the ratio of cycles present in the time signal to the number of cycles to failure. The Palmgren-Miner rule can therefore be expressed as equation 1.

$$D = \sum_i \frac{N_i}{N_f} \tag{1}$$

D is the fatigue damage ratio. If $D \geq 1$ then the component is likely to fail within the duration of the test. If $D < 1$ then the fatigue life is determined as $^T/_D$ seconds, where T is the duration of the test in seconds. N_i is the number of cycles in the i^{th} bin in the histogram with stress amplitude S_i, and N_f is the number of cycles to failure for that particular stress amplitude.

In this example the fatigue life curve is represented in terms of a SN (or Wöhler) curve. This is often presented as a series of piecewise linear segments in log-space where each segment is represented as equation 2.

$$C = N_f S^b \tag{2}$$

S is the stress amplitude in MPa, N_f is the number of Rainflow cycles to failure, C is the Basquin coefficient (intercept of the SN curve with the Stress axis) and b is the Basquin exponent (gradient of the SN curve in log space). The fatigue damage ratio is therefore obtained by substituting equation 2 into equation 1 as given in equation 3.

$$D = \frac{1}{C} \sum_i N_i \, S_i^b \tag{3}$$

where S_i is the stress amplitude of the i^{th} fatigue cycle in the time signal.

New spectral SN fatigue method

Spectral fatigue proceeds in a manner similar to the time-domain except that the Rainflow cycle counting algorithm is replaced with one based on a Probability Density Function (PDF) of stress amplitude; for example, the Rayleigh, Dirlik or Lalanne PDFs. The end result of the PDF methods is shown as a Rainflow histogram and equation 3 is replaced with equation 4.

$$D = \frac{E_p T}{C} \int_0^\infty p\,(S)\; S^b dS \tag{4}$$

$p(S)$ is the PDF of fatigue cycles, E_p is the expected number of fatigue cycles per second of test exposure and T is the test exposure time in seconds.

Using moments of area under the PSD, Rice [9] derived formulae to estimate the number of peaks per second, E_p, as well as the number of zero up-crossings per second E_0. These are given in equation 5.

$$E_0 = \sqrt{\frac{m_2}{m_0}}$$

$$E_p = \sqrt{\frac{m_4}{m_2}} \tag{5}$$

m_0, m_2 and m_4 are the $0^{th}, 2^{nd}$ and 4^{th} moments of the PSD about the zero Hz axis. The n^{th} moment of area is defined by equation 6. (Note: m_0 is equal to the area under the PSD which also represents the 'mean square' value of the time signal or the square of the RMS)

$$m_n = \int_0^\infty f^n \; G(f) df \tag{6}$$

$G(f)$ is the single sided PSD of stress amplitude at frequency fHz.

A reliable measure of bandwidth was also offered by Rice [9] as a ratio of the number of zero up-crossings in a time signal to the number of peaks. This ratio is often known as the 'irregularity factor γ' and is given by equation 7. For narrow-band signals the irregularity factor tends to one (all peaks occur above the mean) whereas for white noise it tends to $\sqrt{\frac{5}{9}}$.

$$\gamma = \frac{E_0}{E_p} = \frac{m_2}{\sqrt{m_0 m_4}}$$

(7)

In the case of sine-on-random loading, the moments of area of the PSD are adapted to include the effects of the sine terms as shown in equation 8.

$$m_n = \int_0^\infty f^n \; G(f)df + \frac{1}{2}\sum_j F_j^n \, A_j^2$$

(8)

F_j and A_j are the frequency and amplitude of the j^{th} sinusoidal term respectively. (The purpose of the term $\frac{1}{2}\sum A^2$ is to determine the mean-square amplitude of the sine tones.)

For the purposes of this paper, the PDF of fatigue cycles $p(S)$ for a sine-on-random spectrum is given by Rice [9] as equation 9.

$$p(s) = s\int_0^\infty x \; e^{-\frac{(\sigma_r \, x)^2}{2}} J_0(x\, s) \prod_j J_0\,(x\, A_j)dx$$

(9)

s is the stress amplitude in MPa, σ_r is the RMS of the random part of the loading given as the area under the PSD, A_j is the amplitude of the j^{th} sine tone and $J_0()$ is the Bessel function of the first kind of order zero.

Equation 9 is based on the PDF of peaks for the particular case where noise and sine tones are within the same frequency range. Furthermore, the sine tone frequencies are assumed to be incommensurable. In this case the sine tone frequencies must be irrational relative to each other. This means that they can be considered independent and their relative phase has no importance.

The Rainflow amplitude of a fatigue cycle is defined as $\frac{1}{2}(peak - valley)$ so in using equation 9, an implicit assumption is made that each peak is paired with a valley of the same amplitude. This assumption is true for the case of narrow-band signals but can lead to some conservatism in the case on broad-band signals as observed by Rychlik [16].

Closed form solutions exist for the integral in equation 9 when one or no sine tone are present, however a numerical solution is required in the case of multiple tones.

The importance of the deterministic part relative to the stochastic part of the spectrum is given by the sine-to-random power ratio a_0^2 as given in equation 10.

$$a_0^2 = \frac{\sigma_s^2}{\sigma_r^2} = \frac{1}{2\sigma_r^2}\sum_j A_j^2 \tag{10}$$

where σ_s is the RMS of the combined sine waves.

Swept-sine-on-random loading

Whereas sine-on-random vibration excitation is seen during constant-speed rotation, swept-sine-on-random excitation is seen during variable-speed rotation. A pragmatic solution to the case of swept-sine loading is to take advantage of the fact that the sweep rate frequency is very low when compared with the lowest vibration test frequency and the first mode natural frequency of the test component. This permits an approach where the swept-sine-on-random signal can be discretised into a number of individual sine-on-random tests. The damage from a unit exposure time to each sine-on-random test is computed using the above method. Each sine-on-random test is then weighted by the sweep duration over that corresponding interval, and the resulting damage is summed using the Palgren-Miner linear damage accumulation law.

The approach described here offers a significant improvement in analysis time over the case of time-domain simulation because the relatively slow sweep rates would demand a very long time signal be generated.

CASE STUDY

Components and equipment attached to, or placed on, a helicopter must comply with vibration standards. These vibration standards are specified by the aircraft manufacturer as well as other standards such as; the US military standard MIL-STD-810G [1], the UK military standard Def Stan 00-35 [2] and the civil aviation standard RTCA/DO160G [3]. Depending on the location of the component, these standards define the vibration qualification tests that are required in order to certify the components over a specified life expressed in flying hours.

The vibration tests usually consist of the following steps and these can be in various formats, such as; swept-sine, sine-dwell, sine-on-random and PSD random.

1. Initial functionality test.
2. Initial resonance search.
3. Endurance test.
4. Final resonance search.
5. Final functionality test.

The purpose of the initial functionality test is to ensure that equipment is able to function properly in the vibration environment. The initial resonance search ensures that no

significant structural mode is excited by a principal vibration frequency of the aircraft, for example, a harmonic of the blade rotor frequency. The endurance test exposes the equipment to an entire life-time's worth of vibration damage over a highly accelerated time frame. The final resonance search ensure that no changes are apparent in the resonant response of the equipment that could be indicative of a progressive structural failure. And the final functionality test ensures that the equipment is still fully functional following the test. Vibration testing can be expensive and it is therefore useful to simulate the test computationally in order to avoid foreseeable problems.

This case study considers an item of equipment mounted externally on a helicopter. The equipment failed under the specified endurance test. The failure was thought to be due to a vibration mode occurring close to the blade-passing frequency of the helicopter. The equipment supplier therefore wanted advice on the failure mechanism in order to redesign the equipment to achieve the required qualification.

In order to determine if the equipment failed due to fatigue cracking, the vibration test was simulated using nCode DesignLife with MSC Nastran. Two analysis techniques were used. The first considered a frequency-domain simulation using Nastran SOL 111, (modal frequency response), along with the spectral fatigue method described in this paper. The second considered a time-domain simulation using Nastran SOL 112, (modal transient response), along with a time signal reconstruction of the sine-on-random test profile.

Excitation spectrum

The sine-on-random excitation spectrum was derived using MIL-STD-810G. A comparison with service flight loads showed an under-estimate in some ranges of the spectrum and so test tailoring was performed as described by Halfpenny and Walton [17]. The sine-on-random spectrum is illustrated in Fig. 2. A random profile is used between 10 and 500Hz with sine tones applied at harmonics of the blade passing frequency (1nR, 2nR and 3nR). The vertical and lateral accelerations were found to dominate the loading environment, whereas the fore/aft axis is relatively benign. Only the vertical axis is considered in this paper.

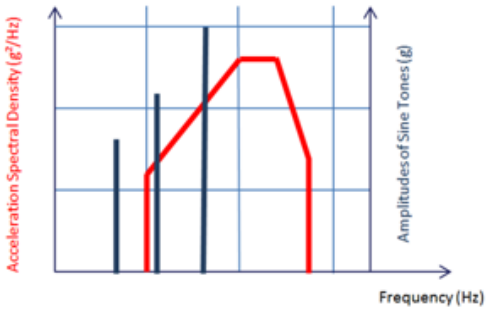

Fig. 2: Sine-on-random excitation spectrum

Stress response

Both a transient dynamic analysis and a frequency response analysis were performed using MSC Nastran. The transient dynamic analysis produces a time series of stress, whereas a frequency response analysis produces a complex frequency response matrix in the modal coordinate system. nCode DesignLife was used to process these data. The analysis consisted of modal summation followed by a multiaxial critical plane fatigue analysis. Using this technique, stresses at each node are resolved on to a rotating axis frame and the axis with the most critical damage is reported. Modal summation was performed in DesignLife in order to reduce the size of data transferred between the two software packages. For the purposes of time-domain simulation, a test signal of 100 seconds was produced at a sample rate of 1024 points per second. A typical time signal of stress response is shown in Fig. 3.

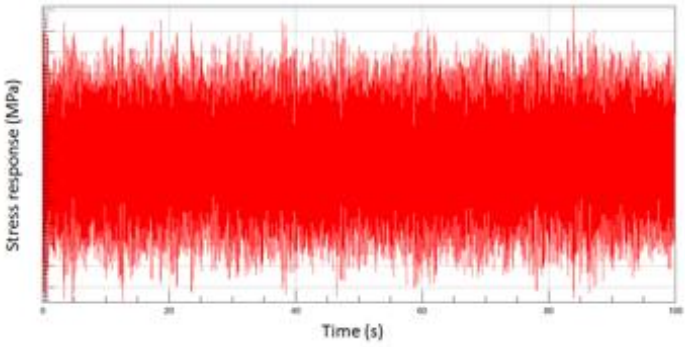

Fig. 3: Typical time signal representation of stress response at node

Fig. 4 shows typical spectral results for two nodes on the model. Fig. 4a illustrates the case of a narrow-banded response excited principally by the random component of the signal, whereas, Fig 4b illustrates the case of a broad-banded response excited significantly by a harmonic of the blade passing frequency. The characteristics of the two responses are summarised in Table 1.

Table 1: Characteristics of the two responses.

Location	Sine to power ratio a_0^2	Irregularity factor γ
a	1.2	0.98
b	8.2	0.87

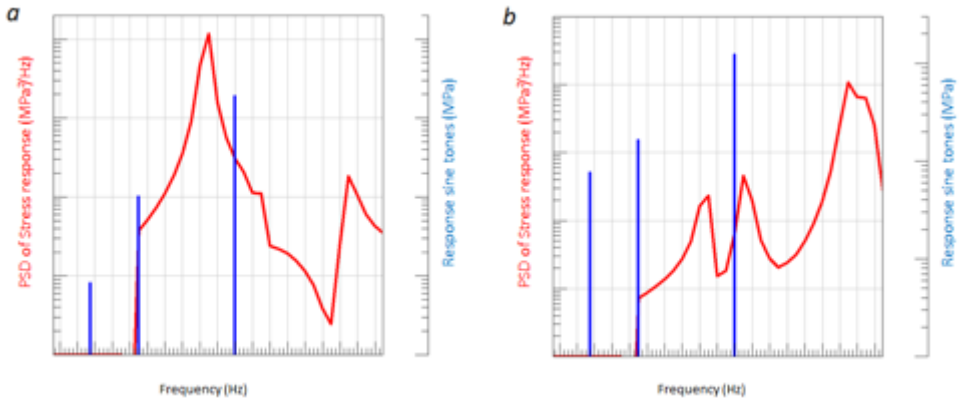

Fig. 4: Sine-on-random stress response spectrum at two locations, a and b, on the component.

Rainflow cycle distributions and fatigue life estimation

Fig. 5 compares the rainflow cycle histogram obtained from the time-domain solution (red) with that obtained using the spectral approach (blue) for both critical locations on the model.

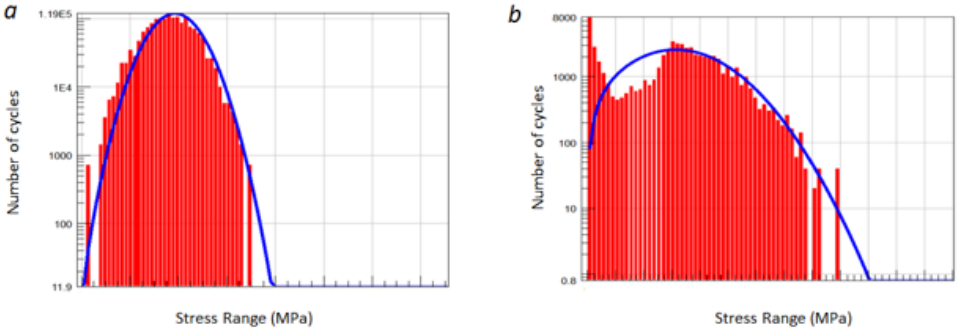

Fig. 5: Comparison between rainflow cycles using the time-domain (red) and spectral (blue) approaches.

With reference to Table 1, location a: we observe from the irregularity factor, $\gamma = 0.98$, that the stress response at this location is relatively narrow-banded and from the sine to power ratio, $a_0^2 = 1.2$, that the influence of the sine tones is approximately the same as the random noise. From Fig. 4a, the response could be described as a single mode response that is excited by the random vibration portion of the sine-on-random signal. With exception of the lowest frequency sine tone, which is of relatively low amplitude, the dominant sine tones lie within the frequency range of the random noise. Furthermore, the sine tone

frequencies are associated with harmonics of the blade passing frequency and so occur at multiples of each other. Therefore location *a* does not respect strictly the assumptions made in the derivation described in this paper. However, the derived stress PDF shown in Fig. 5a still shows excellent correlation with the rainflow histogram obtained through rainflow cycle counting in the time-domain. The time-domain simulation used here was limited to a duration of 100 seconds because of the high computational effort. It is likely that this has curtailed some of the high amplitude cycles, seen at the right of the histogram, that would otherwise have occurred in a longer signal.

With reference to Table 1, location *b*: we observe from the irregularity factor, $\gamma = 0.87$, that the stress response at this location is relatively broad-banded and from the sine to power ratio, $a_0^2 = 8.2$, that the influence of the sine tones is dominant. From Fig. 4b, the response could be described as a multi-modal response where the second structural mode is excited by the second sinusoidal harmonic. This situation will highlight further the effect of the assumptions made in the method's derivation. However, the resulting stress PDF shown in Fig. 5b still shows excellent correlation with the rainflow histogram obtained through rainflow cycle counting in the time-domain. The sparsely populated rainflow bins at the right of the histogram again highlight the limitations of the time signal duration on properly resolving the higher amplitude cycles.

Table 2 compares the fatigue damage ratio estimates obtained at the two critical locations using both the time-domain and spectral methods.

Table 2: Fatigue damage ratio estimates.

Location	Fatigue damage from time-domain	Fatigue damage from frequency-domain	Discrepancy
a	16E-3	23E-3	44%
b	26E-3	36E-3	38%

The fatigue damage estimates given in Table 2 show excellent correlation between the two methods. The discrepancy of approximately 40%, which is small in terms of fatigue, shows that the time-domain approach is underestimating the damage when compared with the spectral approach. This is explained because of the sparsely populated rainflow bins towards the right-hand side of the rainflow histogram. If the time signal reconstruction were made much longer, then more cycles would be observed at the extreme ranges thereby increasing the fatigue damage. In this case the spectral approach is considered more representative and reliable than the time-domain.

The final fatigue life estimates were found to be within a factor of 2 of the number of hours of testing to cause the crack. Under these circumstances, such an accurate result is acknowledged to be somewhat down to chance.

CONCLUSION

A spectral approach to fatigue analysis offers advantages over the time-domain approach when limited stress time history data are available or computation times are prohibitive. A very robust method of deriving fatigue estimates for sine-on-random vibration is presented and a method for extending this to also consider swept-sine-on-random is also discussed.

A case study is presented that compares fatigue analysis using the spectral approach with that of the time-domain approach for a component attached to the fuselage of a helicopter. Excellent correlation between the two approaches is demonstrated. In this case study, the results from the spectral approach are found to be more reliable than those from the time-domain approach. This is because the spectral approach is able to implicitly account for the statistically rare occurrence of high amplitude cycles that only appear over long duration exposure. These cycles are missing from the time signal reconstruction because of the relatively short exposure simulated.

The approach offers an efficient means for 'virtual vibration testing' based on FEA simulation. The benefits of numerical simulation include:

- Pre-test validation – virtual testing can highlight design problems before committing to physical component testing.
- Test optimisation – ensures that the test specification delivers the desired damage in the least amount of time.
- Ensure that the test is not 'over-accelerated', i.e. the sine-on-random amplitude is not excessively severe which could give rise to local plasticity and a change in the failure mode.
- Estimate the residual life, safety margin and confidence levels of a component where physical tests do not run to destruction or where the number of physical tests are limited.
- Estimate the effect of amplitude 'clipping' in the physical test, for example, clipping applied at $\pm 3\sigma$ amplitude.

Before now, the approach for high-cycle fatigue damage assessment under random vibration was limited to Gaussian random loads. The new method extends this to consider the non-Gaussian case where multiple sine tones are superimposed on the Gaussian random loads. This new method is particularly useful for fatigue analysis of components subjected to vibration generated by rotating machinery.

REFERENCES

[1] 2008, *MIL-Std-810g: Test Method Standard for Environmental Engineering Considerations and Laboratory Tests*, United States Department of Defense.

[2] *Def Stan 00-35: Environmental Handbook for Defence Materiel, Part 3: Environmental Test Methods.*, UK Ministry of Defence.

[3] 2010, *RCA/Do-160 Revision G: Environmental Conditions and Test Procedures for Airborne Equipment*, RTCA.

[4] Bendat, J., 1964, *Probability Functions for Random Responses*, NASA report on contract NAS-5-4590.

[5] Steinberg, D., 2000, *Vibration Analysis for Electronic Equipment*, Wiley-Interscience.

[6] Dirlik, T., 1985, "Application of Computers in Fatigue Analysis," PhD thesis, University of Warwick, UK.

[7] Bishop, N., and Sherratt, F., 1989, "Fatigue Life Prediction from Power Spectral Density Data," Environmental Engineering, **2**.

[8] Lalanne, C., 2009, *Mechanical Vibration and Shock Analysis, Fatigue Damage*, Wiley.

[9] Rice, S., 1944, "Mathematical Analysis of Random Noise," Bell System Technical Journal, **23**, pp. 282–332.

[10] Halfpenny, A., and Kihm, F., 2010, "Rainflow Cycle Counting and Acoustic Fatigue Analysis Techniques for Random Loading."

[11] Matsuishi, M., and Endo, T., 1968, "Fatigue of Metals Subjected to Varying Stress."

[12] Downing, S., and Socie, D., 1982, "Simple Rainflow Counting Algorithms," Int. J. Fatigue, **4**(1), pp. 31–40.

[13] Goodman, J., 1899, *Mechanics Applied to Engineering*, Longman, Green & Company, London.

[14] Palmgren, A., 1924, "Die Lebensdauer von Kugellagern (the Service Life of Bearings)," Zeitschrift des vereinesdeutscher ingenierure (Magazine of the Association of German Engineers), **68**(14), pp. 339–341.

[15] Miner, M., 1945, "Cumulative Damage in Fatigue," J. Appl. Mech., **67**, pp. A159–A164.

[16] Rychlik, I., 1993, "On the 'Narrow-Band' Approximation for Expected Fatigue Damage," Probab. Eng. Mech., **8**, pp. 1–4.

[17] Halfpenny, A., and Walton, T., 2010, "New Techniques for Vibration Qualification of Vibrating Equipment on Aircraft."

Corresponding author: andrew.halfpenny@hbmprenscia.com